

行政院國家科學委員會專題研究計畫 成果報告

哺乳類精子獲能作用相關之磷化酪蛋白之訊號傳遞研究

計畫類別：個別型計畫

計畫編號：NSC91-2320-B-038-029-

執行期間：91年08月01日至92年07月31日

執行單位：臺北醫學大學生物化學科

計畫主持人：黃彥華

報告類型：精簡報告

處理方式：本計畫涉及專利或其他智慧財產權，2年後可公開查詢

中 華 民 國 92 年 10 月 29 日

# 行政院國家科學委員會專題研究計畫 成果報告

## 哺乳類精子獲能作用相關之磷化酪蛋白之訊號傳遞研究

計畫類別：個別型計畫

計畫編號：NSC 91 - 2320 - B - 038 - 029

執行期間：91 年 08 月 01 日 至 92 年 07 月 31 日

執行單位：臺北醫學大學生物化學科

計畫主持人：黃彥華 助理教授

### **SVA/SVDF Inhibit PAF-Induced Mouse Sperm Capacitation and Protein Tyrosine Phosphorylation**

#### **INTRODUCTION**

Platelet-activating factor, 1-O-alkyl-2-O-acetyl-sn-glycero-3-phosphorylcholine, is a novel potent signaling phospholipid, it was first described to trigger platelet activation (1), and PAF has a significant role in reproduction, including ovulation, fertilization, preimplantation embryo development, implantation and parturition (2). The presence of PAF in spermatozoa has been reported in various mammalian species including mouse, rabbit, cattle, and human (3-6), and PAF receptor is localized in the midpiece and proximal head of human and mouse spermatozoa by immunofluorescence (7,8). It has been reported that addition of exogenous PAF could induce sperm capacitation, acrosome reaction (AR), and in vitro fertilization in mouse, rabbit and human (9-12), and further increase the motility of fresh and cryopreserved human spermatozoa (13,14); however, it was blocked by PAF receptor antagonist (15).

It was well known that seminal vesicle contains decapacitation activity (16), and removal of seminal plasma is required for capacitation. It was proposed that

lipid-dense vesicles within the seminal plasma denote cholesterol to the sperm membrane, preventing capacitation, and our previous report a protein in seminal plasma, we named as seminal vesicle autoantigen (SVA), now we rename it as seminal vesicle decapacitation factor (SVDF), play the decapacitation effect to inhibit BSA induced mouse sperm capacitation in vitro. Here, we demonstrated SVDF is a decapacitation factor again by: First, SVDF could bind to PAF, and the apparent K<sub>d</sub> of SVDF-PAF complex was estimated as around 10<sup>-5</sup>M. Second, SVDF could suppress the PAF-induced sperm capacitation and protein tyrosine phosphorylation.

## **MATERIALS AND METHODS**

### ***Materials***

Aluminum-backed silica gel-thin layer chromatogram (TLC) plates were purchased from Whatman (Maidstone, England). Bovine serum albumin (BSA) free from fatty acid, chlortetracycline (CTC), phosphatidylcholine (PtdCho), lysophosphatidylcholine, phosphatidylethanolamine (PtdEtn) from egg yolk lectin; PtdIns from pig liver, phosphatidylserine (PtdSer) and sphingomyelin (SPM), platelet-activating factor (PAF, 1-O-alkyl-2-O-acetyl-sn-glycero-3-phosphorylcholine), lyso-PAF, polyvinylalcohol, phosphomolybdic acid spray and Dragendorff reagent were purchased from Sigma Chemical Co. (St. Louis, MO). Anti-mouse IgG horseradish peroxidase (HRP) conjugate was purchased from Promega. Antiphosphotyrosine monoclonal antibody (clone 4G10) was from UBI Co. (Lake Placid, NJ). Chemiluminescence detection ECL plus and Percoll were from Amersham Pharmacia biotech. (Buckinghamshire, UK). PD-10 columns were obtained from Pharmacia (Uppsala, Sweden). Poly(isobutyl methacrylate)

was obtained from Aldrich (Milwaukee, WI, U.S.A). All chemicals were of reagent grade.

### *Preparation of Spermatozoa*

The culture medium used throughout these studies was the modified HM which contained 120.0 mM NaCl, 2.0 mM KCl, 1.20 mM MgSO<sub>4</sub> · 7H<sub>2</sub>O, 0.36 mM NaH<sub>2</sub>PO<sub>4</sub>, 15 mM NaHCO<sub>3</sub>, 10 mM HEPES, 5.60 mM Glucose, 1.1 mM sodium pyruvate, 1.7 mM CaCl<sub>2</sub>, 1mg/ml polyvinylalcohol, 100 I.U./ml penicillin, 100 µg/ml streptomycin. In accordance with a previous method [6], the pH of culture medium was adjusted to 7.3 ~ 7.4 by aeration with humidified air / CO<sub>2</sub> (19 : 1) in an incubator at 37 °C for 48 h before use. Polyvinylalcohol was added to serve as a sperm protectant [7].

Adult male mice (12~16 wk) were killed by cervical dislocation. The epididymides were removed and immersed in HM medium. After they were carefully dissected away from the connective tissues, spermatozoa were extruded from the distal portion of the tissues at 37 °C for 10 min. The cells were gently filtered through two layers of nylon gauze, layered on top of a linear gradient of 20 ~ 80 % Percoll, and centrifuged at 275 ×g at room temperature for 30 min [8,9]. Three distinct cell layers were formed. The lowest layer, which contained more than 95 % viable cells with progressive motility, was diluted with three volumes of the medium and centrifuged at 60 ×g for 10 min at room temperature. The cell pellets were resuspended and centrifuged by the same way for two more times. The cell pellets were resuspended in HM medium for further study.

### *Preparation of SVA derivative*

Outbred ICR mice were purchased from Charles River Laboratories (Wilmington, MA, U.S.A.). They were bred in the animal center at the College of Medicine, National Taiwan University. Animals were in accordance with the institutional guidelines for the care and use of experimental animals. They were

kept under controlled lighting (14 h light/10 h dark) at 21~22 °C with the supply of water and NIH 31 laboratory mouse chow *ad libitum*. SVA I and SVA II were purified from mouse SVS as described previously [5]; they were collected from mature male mice (8~12 wk). SVA I was used throughout the study.

Biotinylated SVA was prepared as described previously [9]. To 490 µl of 20.4 µM SVA in 0.1 M NaHCO<sub>3</sub> containing 0.2 M NaCl at pH 8.3, 10 µl of 20 mM BNHS in DMF was added; the molar ratio of reagent to protein was 20. The mixture was stirred gently at room temperature for 2 h. This reaction was stopped by the addition of 50 µl of ethanolamine. The biotinylated SVA was separated through a PD-10 column that had been preequilibrated with the same buffer. The protein peak was collected, dialyzed against distilled water, freeze-dried and stored at -70 °C before use.

#### *Cytological observation*

CTC staining method of Ward and Storey [10] was exploited to score the population of mouse spermatozoa in the uncapacitated, capacitated and acrosome-reacted stages under a fluorescence microscope.

Coomassie blue staining was performed with the method as described before ( ). Briefly, sperm suspension was washed in PBS twice by a brief centrifugation (2000 rpm, 10 min) and smear on slides, fixed in methanol and air dry. The sperm smear was stained with 0.22 % Coomassie blue G250 in 50 % methanol and 10 % glacial acetic acid for 5 min, and wash in dH<sub>2</sub>O. The spermatozoa with dark blue band over the acrosome region were acrosome-intact, while the ones without blue bands were acrosome-reacted. The percentage of acrosome-reacted spermatozoa (AR %) in at least 200 spermatozoa was scored.

#### *Detection of protein tyrosine phosphorylation in spermatozoa*

After spermatozoa in the modified HM had been incubated at a

specified condition, we followed the previous procedures of Visconti et al [12] to prepare the soluble fraction of cell lysate. Resolution of the protein components in the soluble extract was performed on a 10 % polyacrylamide gel (12 × 10 × 0.075 cm) by the method of Laemmli [13]. The proteins on the gel was transferred to a nitrocellulose membrane by an electrophoretic method of Towbin et al [14], conducting at 30 V for 6 h at 4 °C. After transfer, protein blots were immunodetected by Western blot procedure, using a monoclonal antibody against phosphotyrosine as the primary antibody and anti-mouse IgG conjugated with horseradish peroxidase as the secondary antibody. The enzyme activity staining bands were enhanced by chemiluminescence detection using an ECL kit according to the manufacture's instructions.

### *Fluorescence Spectra*

The fluorescence intensity of SVA in Tris-buffered saline (TBS), expressed in arbitrary units, was measured at room temperature with a Hitachi F-4500 fluorescence spectrophotometer. Both the excitation and the emission slit-widths were 10 nm. Raman emission due to the scattering of solvent was minimized by adjusting the intensity scale. It took no more than 5 min to scan a spectrum, avoiding protein denaturation. The fluorescence intensity at wavelength  $\lambda_2$  (nm) when the fluorophore was excited at wavelength  $\lambda_1$  (nm) is denoted by  $F_{\lambda_1}^{\lambda_2}$ . A modified Scatchard plot [22] was constructed to analyze the fluorescence data of a complex formed by SVA and phosphatidylcholine :

$$(1) \quad \frac{|\Delta F|}{[L]_{\text{free}}} = \frac{F}{K_d} - \frac{|\Delta F|}{K_d}$$

where  $\Delta F$  is the change in protein fluorescence on the adding of ligand,  $L$ ,  $F$  is the protein fluorescence in the absence of ligand, and  $K_d$  is the dissociation constant of the complex. Throughout the titration,  $|\Delta F|/[L]_{\text{total}}$  was plotted against  $|\Delta F|$ , because  $[L]_{\text{free}}$  was close to  $[L]_{\text{total}}$ .

### *TLC-overlay technique*

Binding of SVA-biotin to phospholipids on a TLC plate generally modified the method of Desnoyers and Manjunath [19]. Purified lipids were chromatographed on aluminum-backed silica gel TLC plates in chloroform/methanol/H<sub>2</sub>O (65 : 25 : 4, by vol.). The plates were air-dried and immersed in 0.1 % poly(isobutyl methacrylate) in hexane for 1 min. The chromatograms were dried and blocked for 1 h at room temperature in PBS containing 5 % (v/v) non-fat skim milk. Plates were overlaid with SVA-biotin (2 µg/ml) in the blocking buffer (100µl/cm<sup>2</sup>), incubated for 90 min at 25 °C, washed five times, each 1~2 min, with cold PBS, and then further treated with horseradish phosphatase conjugated streptavidin diluted 1: 1000 in the blocking solution for 1 h. The TLC plate was agitated gently in three changes of cold PBS for 10 min each. The phospholipids associated with the biotinylated SVA that bound to horseradish phosphatase conjugated streptavidin were then subjected to enzyme activity staining by ECL system. The lipids on triplicate plates were also detected by spraying the plates with phosphomolybdic acid solution [20] or Dragendorff reagent [21].

### *Statistical Analysis*

All of the previously mentioned treatments were repeated at least three times on three different pooled spermatozoa from 4 ~ 5 male mice. The analysis was performed by one-way ANOVA.

## **RESULTS**

### *SVA-biotin binding to PAF by TLC overlay technique*

TLC overlay technique was used to identify the PAF/phospholipid interacted with SVA protein. SVA-biotin derivatives were prepared as described in Material and Methods. Several authentic phospholipids, such as

PC, SPM, lysoPC, PAF, PA and lyso PAF were applied on the TLC plate, developed by the organic solvent system and stained with phosphomoybid acid to indicate the phospholipid character as described in our previous report (?). As we expect in Fig.1, PC, SPM, lysoPC shows strong binding to SVA-biotin, and PA was used as the negative control since it does not bind to SVA ( ). PAF and lysoPAF show positive interaction with SVA-biotin, the binding intensity between PAF and lysoPAF are not many differences, indicate that the choline group on the C-2 fatty acid chain of the phospholipid is more important than the C-2 fatty acid chain only in PAF/lysoPAF binding characteristics according the Dragondorf reagent spray.

#### *Fluorescence analysis*

Fluorescence spectra disturb analysis was used to estimate the binding constant of SVA and PAF. Fig. 2 display the emission of 1.6  $\mu\text{M}$  SVA in the absence and/or in the presence of PAF. Excitation was at 295 nm to excite the fluorescence of the two tryptophan residues ( ). SVA contain two tryptophan residues on the protein surface; therefore, SVA exhibits a peak at 345 nm in TBS (Fig. 2, solid line). The presence of 5.0 % (v/v) ethanol in the protein solution did not change the protein fluorescence in either spectral profile or emission intensity (compare the solid and broken lines in Fig. 2), indicating a lack of effect of the organic solvent in the protein solution on the tryptophan status. In contrast, the addition of PAF dissolved in ethanol to final concentration of 40  $\mu\text{M}$  PAF and 0.5 % (v/v) ethanol in the protein solution considerably enhanced the protein fluorescence intensity but the emission peak did not shift (compare the dot-dashed and solid line in Fig. 2). Apparently, PAF interacted with SVA to change the protein's fluorescence. Therefore PAF-SVA binding was probed by the ability of PAF to perturb the protein fluorescence. We fitted



the F345/295 values, obtained by titrating 1.6  $\mu\text{M}$  SVA protein solution with PAF to equ (1). As shown in the inset of Fig. 2, the modified Scatchard plot is curvature, supporting that there are two types of PAF-binding sites on the protein molecule. The apparent  $K_d$  of PAF-SVA binding was estimated as  $( \quad + \quad ) \times 10^{-5} \text{M}^{-1}$  and  $( \quad + \quad ) \times 10^{-4} \text{M}^{-1}$ .

*SVA suppress the PAF-induced sperm capacitation and acrosome reaction*

To determine the effect of SVA on PAF-induced sperm capacitation, sperm ( $10^6$  cells/ml) were suspended in modified Tyrode solution either alone or in the presence of  $10^{-5} \text{M}$  PAF and 0 %, 0.003 %, 0.03 %, 0.1 %, 0.3 % SVA. More than 85 % of the freshly prepared sperm remained uncapacitated (F form), and nearly no acrosome-reacted cells appeared after incubation at 37 °C for 80 min (Fig. 3A, column 1), the population of capacitated cells is increasing after incubation in Tyrode's solution in the dose dependent of PAF (Fig. 3A, column 2 ~ 4). Approximately 54 % of the  $2 \times 10^{-5} \text{M}$  PAF-treated cells were capacitated, but acrosome-reacted cells (AR form) constituted less than 5 % of the total according the CTC staining results. (Fig. 3A, column 4). Addition of SVA to the incubation medium inhibited PAF-induced sperm capacitation in a dose dependent manner. The decapacitation effect of SVA became detectable at a concentration greater than 0.3 % in the cell incubation medium. The greater the SVA concentration in the medium, the greater its inhibition of PAF-induced sperm capacitation (Fig. 3A, column 5 ~ 8). Approximately 25 % of the induced cells remained in the uncapacitated stage (F form) after incubation with  $10^{-5} \text{M}$  PAF and 0.3 % SVA together (Fig. 3A, column 8), suggesting that SVA can inhibit the PAF induced sperm capacitation. The addition of cAMP agonist recovered the inhibition effect of 0.3 % SVA to 60 % capacitated form (B form).

Coomassie blue staining was used to determine the effect of SVA on

the PAF-induced sperm acrosome reaction. Spermatozoa was prepared as described in capacitation assay. In the absence of A23187 ionophore, the control cells remained around 23 % acrosome-reacted (AR %), and the SVA / SVA-cAMP analog treated cells were 30 % and 38 % represently. Addition of PAF from  $2 \times 10^{-7}$  M to  $2 \times 10^{-5}$  M increase the percentage of acrosome reaction from 21 % to 32 %. SVA inhibit the PAF-induced sperm acrosome reaction in a dose dependent manner (Figure 3B, lane ), approximately 20 % of the treated cells remained acrosome-reacted in the presence of  $2 \times 10^{-5}$  M PAF and 3 mg/ml SVA. The addition of cAMP agonist recovered the inhibition effect of 0.3 % SVA from 20 % to 48 % acrosome-reacted form, suggesting that involved a cAMP dependent pathway.

#### *SVA Suppress the PAF-induced the capacitation associated protein tyrosine phosphorylation*

Figure 4 displays the protein tyrosine phosphorylation patterns of epididymal spermatozoa after incubation with  $10^{-7} \sim 10^{-5}$  M PAF or/and 0 % ~ 0.3 % SVA in the modified HM at 37 °C for 90 min. In the control cells, phosphorylation was mainly restricted to a protein band with a molecular mass of approximately 120 kDa, as described by Kalab et al ( ) to be the p95/106 hexokinase (Fig. 4, lane 1). In addition, as described in our previous report ( ), several weak phosphorylated bands appeared in a group of proteins in the range of Mr 40,000 ~ 100,000, and SVA-treated cells appear no other phosphorylated protein except the p95/106 hexokinase (Fig. 4, lane 1 and lane ?). Relative to the protein tyrosine phosphorylation of the control cells, phosphorylation of proteins in the range of Mr 40,000 ~ 100,000 was greatly enhanced in the PAF-treated cells (Fig. 4, lane 2 ~ 4). This was similar to the effect of BSA on the cells reported by Visconti et al ( ). The extent of PAF-induced protein tyrosine phosphorylation was

gradually suppressed as a function of the concentration of SVA (Figure 4, lane 5 ~ 8). Only the p95/106 hexokinase was phosphorylated in the cells incubated with  $10^{-5}$  M PAF and 0.3 % SVA together (Fig. 4, lane 8). Apparently, the protein tyrosine phosphorylation associated with PAF-induced sperm capacitation could be suppressed by the presence of SVA. However, the addition of dbcAMP plus IBMX to the culture medium in the presence of  $10^{-5}$  M PAF and 0.3 % SVA, recovered the suppression effect of SVA on PAF induced protein tyrosine phosphorylation (Fig. 4, lane 9).

*SVA suppress the PAF induced mouse sperm capacitation and protein tyrosine phosphorylation by a cAMP-dependent pathway*

Since it has been demonstrated that cAMP analog, dibutyryl cAMP could accelerate capacitation and protein tyrosine phosphorylation in vitro in mouse sperm ( , ), we examined whether the addition of dbcAMP plus IBMX influenced the time-dependent onset of protein tyrosine phosphorylation that occurs during the normal time course of capacitation in vitro. As shown in Fig. 5, adding of 1mM dbcAMP and 100  $\mu$ M IBMX to the culture medium significantly reduced the time which needed to induced the capacitation-associated protein tyrosine phosphorylation when compared to controls (Fig. 5A and 5B). The addition of SVA to the culture medium in the presence of  $10^{-5}$  M PAF and dbcAMP plus IBMX, delay the time course of protein tyrosine phosphorylation induced by  $10^{-5}$  M PAF and dbcAMP plus IBMX (Fig. 5C). In contrast to PAF, lysoPAF did not show any capacitation and the capacitation associated protein tyrosine phosphorylation patterns of spermatozoa (Fig 5D).

H-89,

N-[2-(p-bromocinnamylamino)ethyl]-5-isoquinolinesulfonamide, is a highly selective and cell permeable inhibitor of PKA (Chijiwa et al,1990). Fig. 6

show that H-89 inhibited the PAF-induced protein tyrosine phosphorylation of sperm in a concentration-dependent manner with a maximal effect at 10  $\mu$ M. In contrast, the protein tyrosine phosphorylation of the p95/116 hexokinase was unaffected by H-89 at all concentration tested.

Figure 1 Biotin-SVA/SVDF TLC-Overlay technique

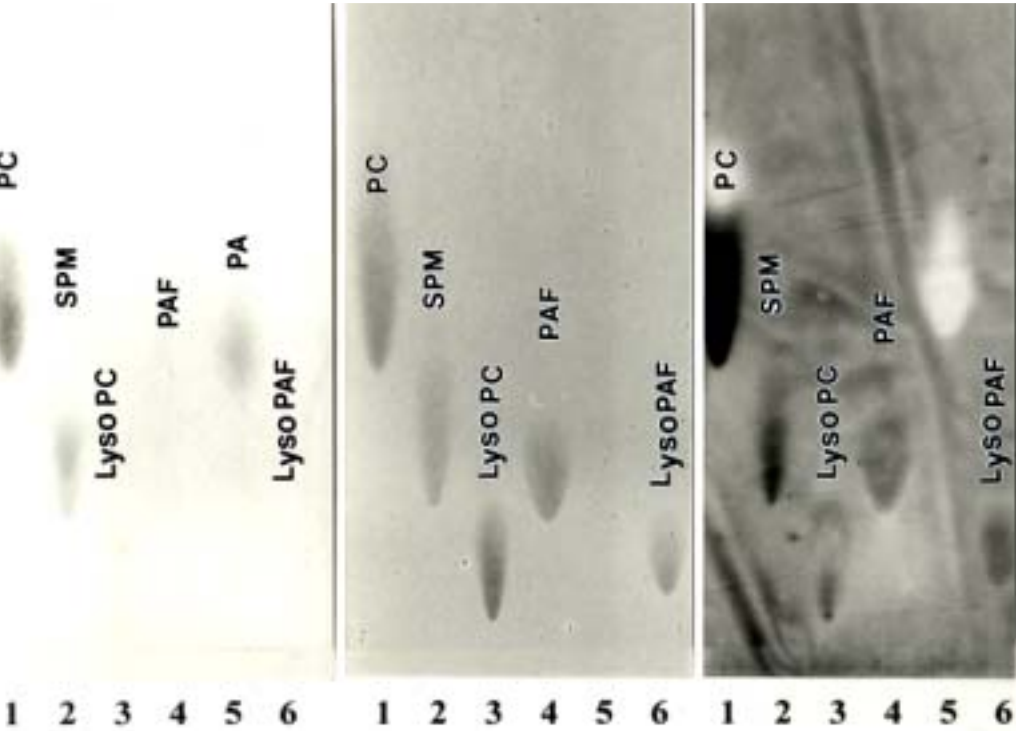
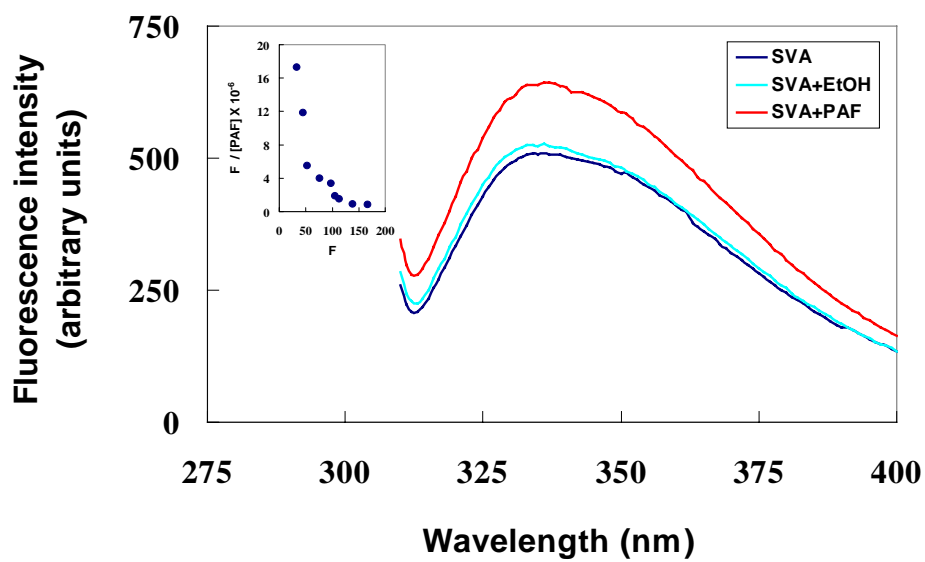
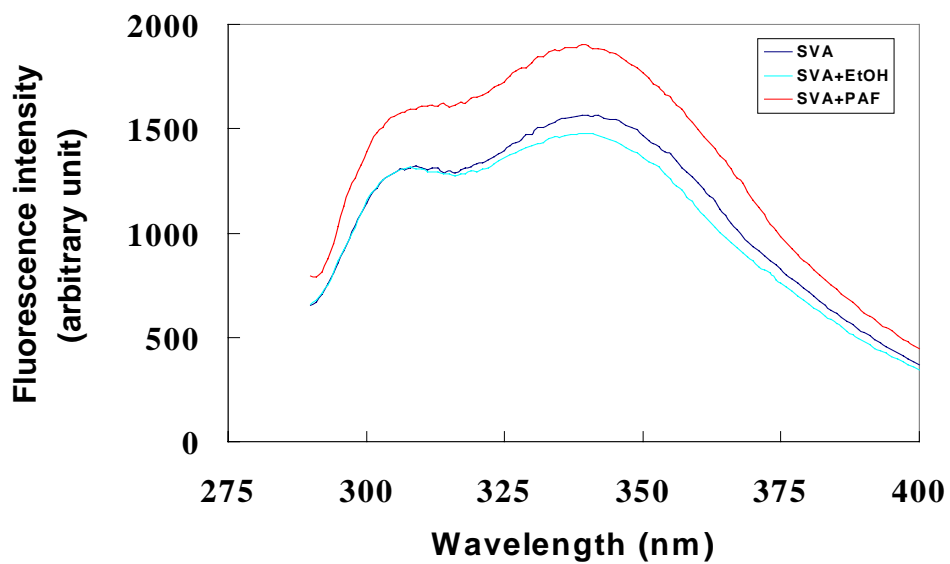
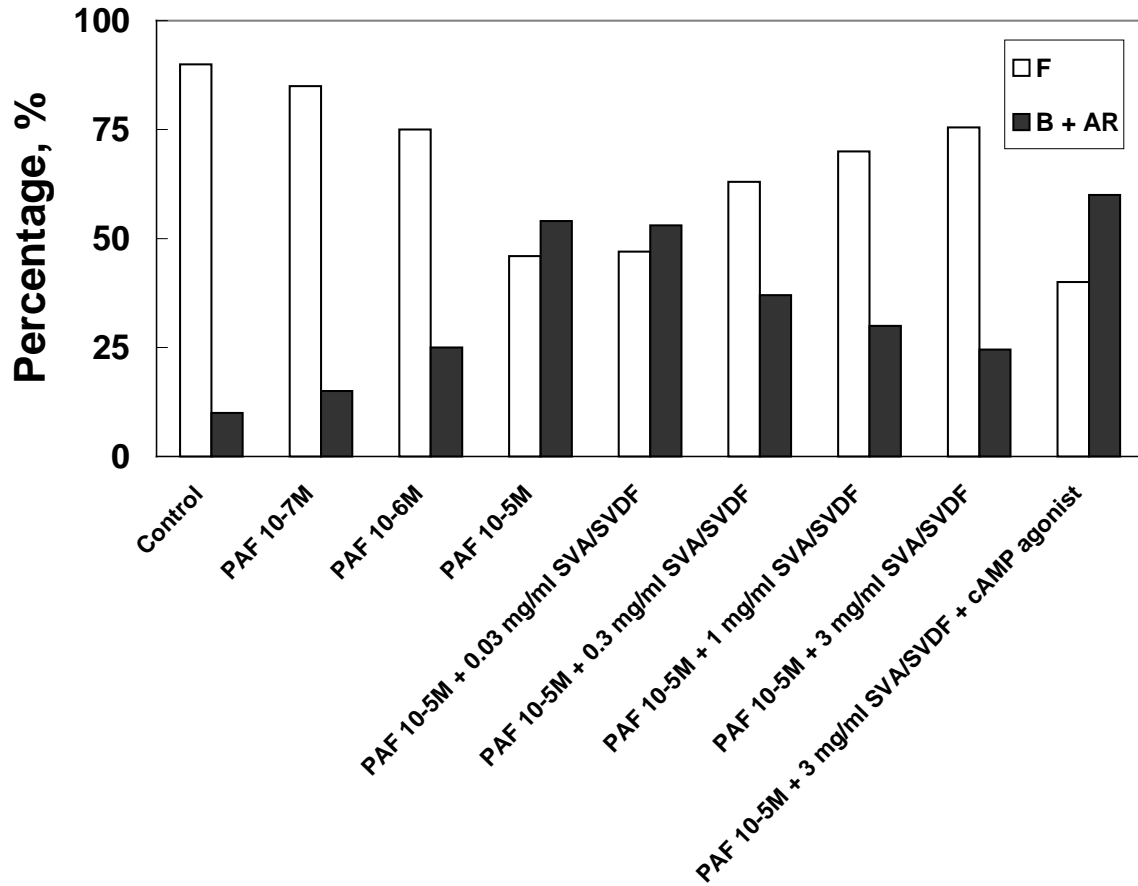


Figure 2 Fluorescence Spectra disturb analysis



**Figure 3 SVA/SVDF suppress the PAF-induced mouse sperm capacitation and acrosome reaction**



**Figure 4A** SVA/SVDF suppress the PAF-induced mouse sperm capacitation associated protein tyrosine phosphorylation

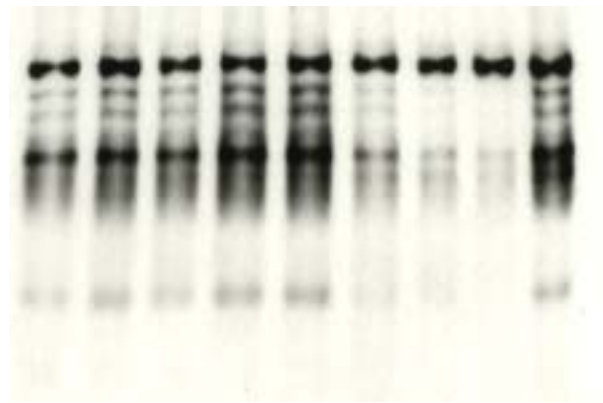
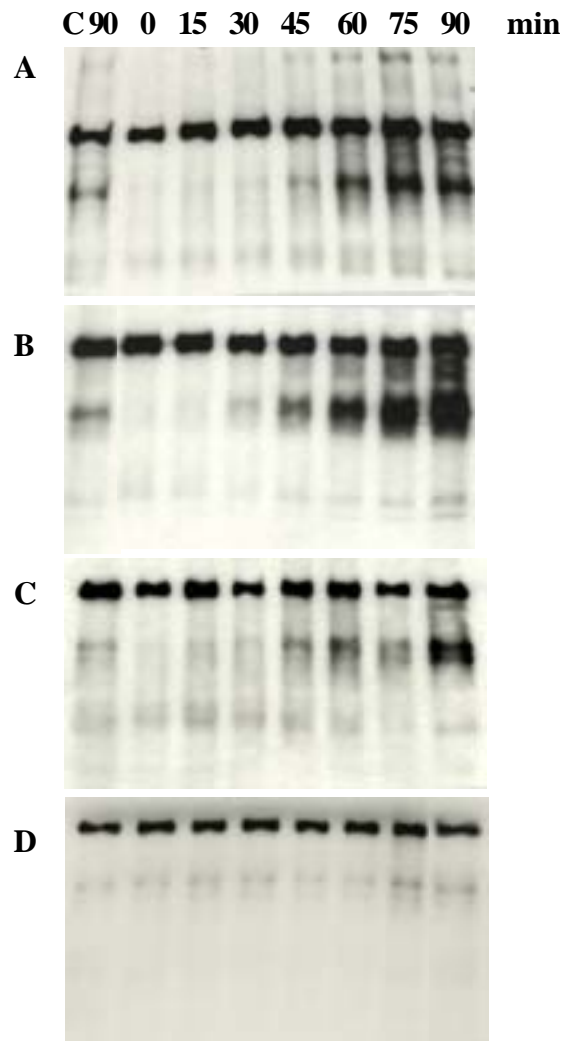


**Figure 4B** H-89, a PKA inhibitor, suppress the PAF-induced mouse sperm capacitation associated protein tyrosine phosphorylation





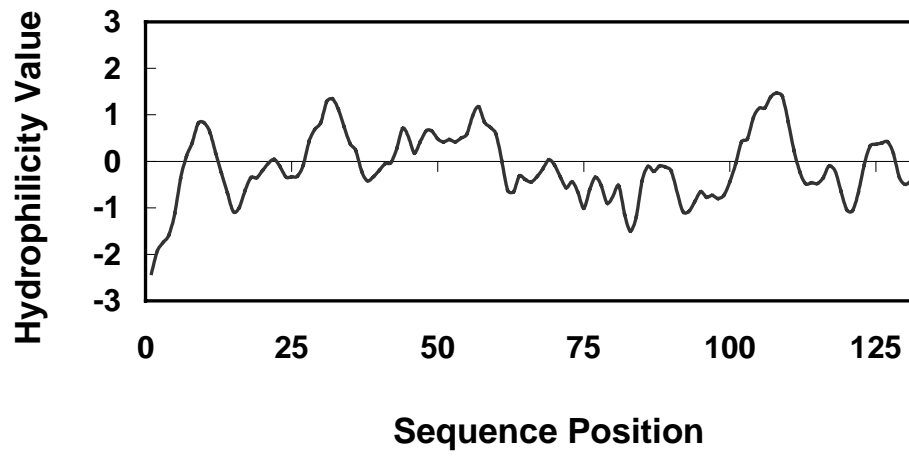
**Figure 5 SVA/SVDF suppress the PAF-induced mouse sperm capacitation and protein tyrosine phosphorylation by a**



**cAMP-dependent pathway**

	0	15	30	45	60	75	90
<b>A</b> $10^{-5}$ M PAF	—	—	—	—			
<b>B</b> $10^{-5}$ M PAF + cAMP	—	—	—				
<b>C</b> $10^{-5}$ M PAF + cAMP + 3mg/ml SVA/SVDF	—	—	—	—	—	—	
<b>D</b> $10^{-5}$ M lysoPAF	—	—	—	—	—	—	—
<b>E</b> 3mg/ml SVA/SVDF	—	—	—	—	—	—	—

**Figure 6 Hydrophobicity of SVA/SVDF protein**



## REFERENCES

1. Chang MC. Fertilizing capacity of spermatozoa deposited into the fallopian tubes. *Nature* 1951; 168: 697-698.
2. Chang MC. Development of fertilizing capacity of rabbit spermatozoa in the uterus. *Nature* 1955; 175: 1036-1037.
3. Austin CR. Observation on the penetration of the sperm into the mammalian egg. *Aust J Sci Res* 1951; 4: 581-596.
4. Austin CR. The "capacitation" of the mammalian sperm. *Nature* 1952; 170: 326.
5. Yanagimachi R. Mammalian fertilization. In: Knobil E, Neill JD (eds.), *The Physiology of Reproduction*. New York. Raven Press, Ltd.;1994: 189-317.
6. Visconti PE, Bailey JL, Moore GD, Pan D, Olds-Clarke P, Kopf GS. Capacitation of mouse spermatozoa. I. Correlation between the capacitation state and protein tyrosine phosphorylation. *Development* 1995; 121: 1129-1137.
7. Benveniste J, Henson PM, Cochrane CG. Leukocyte dependent histamine release from rabbit platelets: The role of Ig-E, basophils, and platelet-activating factor. *J Exp Med* 1972; 136: 1356-76.
8. Hanahan DJ. Platelet activating factor: a biologically active phosphoglyceride. *Annu Rev Biochem* 1986; 55: 483-509.
9. Braquet P, Touqui L, Shen TY, Vargaftig BB. Perspectives in platelet activating factor

- research. *Pharmacol Rev* 1987; 39: 97-144.
10. Harper MJK. Platelet activating factor: a paracrine factor in preimplantation stages of development? *Biol Reprod* 1989; 40: 907-13.
11. Kumar R, Harper MJK, Hanahan DJ. Occurrence of platelet-activating factor in rabbit spermatozoa. *Arch Biochem Biophys* 1988; 260: 497-502
12. Kuzan FB, Geissler FT, Henderson WR Jr. Role of spermatozoa platelet-activating factor in fertilization. *Prostaglandins* 1990; 39: 61-74.
13. Parks JE, Hough S, Elrod C. Platelet activating factor activity in the phospholipids of bovine spermatozoa. *Biol. Reprod.* 1990; 43: 806-811.
14. Minhas BS, Kumar R, Ricker DD, Robertson JL, Dodson MG. The presence of platelet activating factor-like activity in human sperm. *Fertil Steril* 1991; 55: 372-6.
15. Sengoku K, Ishikawa M, Tamate K, Shimizu T. 1992. Effects of platelet activating factor on mouse sperm function. *J Asst Reprod Genet* 9:447-453.
16. Sengoku K, Tamate K, Takaoka Y, Ishikawa M. 1993. Effects of platelet activating factor on human sperm function in vitro. *Hum Reprod* 8:1443-1447.
17. Angle MJ, Tom R, Jarvi K, McClure RD. 1993. Effect of platelet-activating factor (PAF) on human spermatozoa-oocyte interactions. *J Reprod Fertil* 98:541-548.
18. Fukuda A, Roudebush WE, Thatcher SS. 1994. Platelet activating factor enhances the acrosome reaction, fertilization in vitro by subzonal sperm injection and resulting

- embryonic development in the rabbit. *Human Reprod* 9:94–99.
19. Ricker DD, Minhas BS, Kumar R, Robertson JL, Dodson MG. 1989. The effects of platelet activating factor on the motility of human spermatozoa. *Fertil Steril* 52:655–658.
20. Hellstrom WJG, Wang R, Sikka SC. 1991. Platelet-activating factor stimulates motion parameters of cryopreserved human sperm. *Fertil Steril* 56:768–770.
21. Roudebush WE, Fukuda AI and Minhas BS. 1993. Enhanced embryo development of rabbit oocytes fertilized in vitro with platelet activating factor (PAF)-treated spermatozoa. *J Assist. Reprod. Genet* 10:91–94.
22. Roudebush WE, Minhas BS, Ricker DD, Palmer TV, Dodson MG. 1990. Platelet activating factor enhances in vitro fertilization of rabbit oocytes. *Am J Obstet Gynecol* 163:1670–1673.
23. Tjoelker, LW, Eberhardt C, Unger J, Trong HL, Zimmerman G, McIntyre TM, Stafforini DM, Presscott SM, and Gray PW. 1995. Plasma platelet-activating factor acetylhydrolase is a secreted phospholipase A2 with a catalytic triad. *J. Biol. Chem.* 270 : 25481 – 25487.
24. Parks JE and Hough SR. 1993. Platelet-activating factor acetylhydrolase activity in bovine seminal plasma. *J Androl.* 14: 335-339.
25. Muguruma K and Johnston JM. 1997. Metabolism of platelet-activating factor in rat

- epididymal spermatozoa. *Biol. Reprod.* 56: 529-536.
26. Honda Z, Nakamura M, Miki I, Minami M, Watanabe T, Seyama Y, Okado H, Toh H, Ito K, Miyamoto T, and Shimizu T. 1991 *Nature* 349: 342-346.
27. Reinhardt JC, Cui X, Roudebush WE. 1999. Immunofluorescent evidence of the platelet activating factor receptor on human spermatozoa. *Fertil Steril* 71:941-942.
28. Wu C, Stojanov T, Cham O, Ishii S, Shimizu T, Li A, O'Neill C. Evidence for the autocrine induction of capacitation of mammalian spermatozoa. *J. Biol. Chem.* 2001; 276: 26962-26968.
29. Bedford JM and Chang MC. Removal of decapacitation factor from seminal plasma by high speed centrifugation. *Am J Physiol.* 1962, 202:179-181.
30. Davis BK. Interaction of lipids with the plasma membrane of sperm cells. I. The antifertilization action of cholesterol. *Arch Androl.* 1980 Nov;5(3):249-54.
31. Davis BK. Timing of fertilization in mammals: sperm cholesterol/phospholipid ratio as a determinant of the capacitation interval. *Proc Natl Acad Sci U S A.* 1981; 78 :7560-4.
32. Huang YH, Luo CW, Yu LC, Chu ST, Chen YH. The protein conformation and a zinc binding domain of an autoantigen from mouse seminal vesicle. *Biophys J* 1995; 69: 2084-2089.
33. Huang YH, Chu ST, Chen YH. Seminal vesicle autoantigen, a novel phospholipid-binding

protein secreted from luminal epithelium of mouse seminal vesicle, exhibits the ability to

suppress mouse sperm motility. *Biochem J.* 1999; 343: 241-248.

34. Bellvé AR, Zheng W, Martinova YS. Recovery, capacitation, acrosome reaction, and

fraction of sperm. *Methods Enzymol* 1993; 225:113–137.

35. Bavister, B. D. Substitution of a synthetic polymer for protein in a mammalian gamete

culture system. *J. Exp. Zool.* 1981; 217: 45–51

36. ,

37. ,

38. Yu LC, Chen JL, Tsai WB, Chen YH. Primary structure and characterization of an

androgen-stimulated autoantigen purified from mouse seminal-vesicle secretion. *Biochem J*

1993; 296 :571-576

39. Bayer EA, Wilchek M. Protein biotinylation. *Methods Enzymol* 1990;184:138-160.

40. Ward CR, Storey BT. 1984. Determination of the time course of capacitation in mouse

spermatozoa using a chlortetracycline fluorescence assay. *Dev Biol* 104:287–296.

41. , Coomassie blue staining

42. Laemmli UK. Cleavage of structural proteins during the assembly of the head of

bacteriophage T4. *Nature* 1970; 227:680–685.

43. Towbin H, Staehelin TH, Gordon J. Electrophoretic transfer of proteins from polyacrylamide gels to nitrocellulose sheets: procedure and some application.

*Proc Natl*

Acad Sci USA 1979; 76:4350–4354.

44. Epstein, M., Levitzki, A. and Reuben, J. Binding of lanthanides and of divalent metal ions

to porcine trypsin. *Biochemistry* 1974; 13: 1777–1782.

45. Desnoyers, L. and Manjunath, P. Major proteins of bovine seminal plasma exhibit novel

interactions with phospholipid. *J. Biol. Chem.* 1992; 267: 10149–10155.

46. Usui, T. (1963) *J. Biochem. (Tokyo)* **54**, 283–286

47. Wagner, H., Hörhammer, L. and Wolff, P. (1961) *Biochem. Z.* **334**, 175–184

48. Kalab P, Visconti P, Leclerc P, Kopf GS. p95, the major phosphotyrosine-containing

protein in mouse spermatozoa, is a hexokinase with unique properties. *J Biol Chem.* 1994

269: 3810-3817.

49. Huang YH, Chu ST, Chen YH. A seminal vesicle autoantigen of mouse is able to suppress

sperm capacitation-related events stimulated by serum albumin. *Biol Reprod* 2000; 63:

1562-1566.

50. Chijiwa T, Mishima A, Hagiwara M, Sano M, Hayashi K, Inoue T, Naito K, Toshioka T,

Hidaka H. Inhibition of forskolin-induced neurite outgrowth and protein phosphorylation by

a newly synthesized selective inhibitor of cyclic AMP-dependent protein kinase, N-[2-(p

bromocinnamylamino)ethyl]-5-isoquinolinesulfonamide (H-89), of PC12D

pheochromocytoma cells. *J Biol Chem* 1990; 265: 5267-72.

51. Visconti PE, Moore GD, Bailey JL, Leclerc P, Connors SA, Pan D, Olds-Clarke P, Kopf GS.



Capacitation of mouse spermatozoa. II. Protein tyrosine phosphorylation and capacitation

are regulated by a cAMP-dependent pathway. *Development* 1995; 121: 1139-1150.

## Legends

### **Fig. 1 Binding of biotin-SVA/SVDF to PAF separated by TLC**

30 µg of each of the purified phospholipids were spotted and chromatographed on silica-gel TLC plates in chloroform/methanol/water (65 : 25: 4, by vol.). (A) Phospholipids detected with phosphomolybdic acid spray. (B) Choline-containing phospholipids detected with Dragendorff reagent spray. (C) Binding of biotin-labelled SVA/SVDF to separated phospholipids obtained after a TLC-overlay binding technique described in the text. Abbreviations : lyso PA, lysophosphatidic acid ; lyso PC, lysophosphatidylcholine ; PA, phosphatidic acid ; PC, PtdCho ; PE, PtdEtn ; PAF, platelet activating factor; lysoPAF, lyso-platelet activating factor.

### **Fig. 2 Effect of PAF on the fluorescence of SVA/SVDF**

The emission spectra were scanned with excitation wavelength at 275 nm (Fig. 2A) or 295 nm (Fig. 2B). The SVA/SVDF protein was at 6.5 µM in TBS, pH 7.4. Protein alone, broken line, 5 % (v/v) ethanol in the protein solution; dot-dashed line, 40 µM PAF and 1 % (v/v) ethanol in the protein solution. The modified Scatchard plot for the binding of PAF to SVA/SVDF is given in the inset. The data of from adding PAF to the protein solution were analyzed by using Eq. 1 with linear-regression fitting. The correlation coefficient was calculated to be more than ?.

### **Fig. 3 Suppression of PAF-induced sperm capacitation by SVA/SVDF**

Fresh spermatozoa in modified Tyrode solution ( $10^6$  cells/ml) were incubated with  $10^{-7} \sim 10^{-5}$  M PAF in the presence of SVA/SVDF at a final concentration of 0 ~ 3 mg/ml and cAMP agonist. Incubation was conducted in 5% CO<sub>2</sub> in an incubator at 37°C for 80 min. The CTC fluorescence method described in the text

was exploited to score the population of uncapacitated cells (F form, open bars), capacitated cells and acrosome-reacted cells (B + AR form, solid bars). Data represent the means of five individual trials counting 200 cells/treatment per trial, and error bars represent the SD. \*, P, 0.05; \*\*, P, 0.01; and \*\*\*, P, 0.001 in the paired statistical comparison with the corresponding control values being evaluated using one-way ANOVA.

**Fig. 4 Suppression of PAF-induced sperm capacitation-related protein tyrosine phosphorylation by SVA**

The cells ( $5 \times 10^6$  cells/ml) in modified HM were incubated in the presence of PAF and / or SVA/SVDF and cAMP agonist at 37 °C for 90 min (Fig. 4A), and H-89, a protein kinase A inhibitor, (Fig.4B). The soluble fraction of the cell lysate was resolved by SDS-PAGE on a 10% gel slab. The phosphotyrosine of a protein on the gel was immunodetected by a Western blot procedure as described in the text.

**Fig. 5. SVA/SVDF suppress the PAF-induced mouse sperm capacitation and protein tyrosine phosphorylation by a cAMP-dependent pathway**

**Fig. 6 Hydrophobicity of SVA/SVDF Protein**